Synthesis of Vapor-Grown Carbon Fibers Using Nanocrystalline $Fe_{75}Si_{15}B_{10}$ Alloy as a Catalyst*

Ken Unno[1, †], Hidehiro Kudo[1, †], Atsunori Kamegawa[1], Hitoshi Takamura[1],
Masuo Okada[1], Reijiro Takahashi[2] and Junichiro Yagi[2]

[1]*Department of Materials Science, Graduate School of Engineering, Tohoku University, Sendai 980-8579, Japan*
[2]*Institute for Advanced Materials Processing, Tohoku University, Sendai 980-8577, Japan*

The synthesis of vapor-grown carbon fibers (VGCFs) using the nanocrystalline $Fe_{75}Si_{15}B_{10}$ alloy as a novel catalyst has been investigated, and the growth process of VGCFs was discussed. The nanocrystalline $Fe_{75}Si_{15}B_{10}$ alloy with fine bcc-Fe grains less than about 20 nm was prepared by the melt spinning technique followed by annealing. VGCFs with a diameter of less than about 40 nm were successfully prepared using the nanocrystalline $Fe_{75}Si_{15}B_{10}$ catalyst at 773 K under 80%CO–20%H_2 atmosphere. High-resolution transmission electron microscopic characterization indicated that the VGCFs catalytically generated over the $Fe_{75}Si_{15}B_{10}$ nanocrystal surfaces at both 773 K and 873 K most likely have a tubular-type structure, in which the graphite sheets were stacked parallel to the fiber axis. The $Fe_{75}Si_{15}B_{10}$ catalyst particles appear to be made of the single-phase Fe_3C grains, which is in contrast to the $Fe_{91}Zr_7B_2$ catalyst particles previously studied by us. The formation of Fe_3C leads to the brittleness of catalyst particles and results in a growth of filamentous carbon.

1. Introduction

Vapor-grown carbon fibers (VGCFs) can be grown from the catalytic decomposition of certain hydrocarbons or CO gas passing through over heated metal particles such as Fe, Ni, Co, and some of their alloys. It is well known that the structure of the VGCFs depends on the composition of catalysts, reactant gas, synthesis temperature, and other experimental conditions.[1,2] Furthermore, the diameter of the VGCFs is governed by that of the catalyst particles responsible for their growth. Thus, a coprecipitation technique followed by the reduction of metal carbonates is usually employed to prepare the catalyst, since, by which, fine metal or alloy catalysts with a diameter of less than 100 nm can be obtained.

Instead of the conventional coprecipitation technique, the present authors have reported that nanocrystalline Fe–Zr–B alloys can be used as the catalyst for VGCFs growth.[3] The Fe–Zr–B alloy exhibits nanoscale bcc-Fe grains with a diameter of $15 \sim 20$ nm by annealing the as-quenched amorphous phase. In the previous work, we tried to obtain the fine VGCFs with a width of $15 \sim 20$ nm. But, VGCFs with a width ranging widely from 50 to 300 nm were prepared at 873 K under 80%CO–20%H_2. From HREM observations, it was found that each VGCF was grown from a catalyst particle made up from some bcc-Fe grains, and the size of the particles regulated a width of VGCFs. In this work, to control a diameter of VGCFs and understand the role of constituent elements, the Fe–Si–B alloy was employed as a catalyst, which brings nanoscale bcc-Fe grains similar to the Fe–Zr–B alloy.

Thus, the purpose of this study is to prepare the VGCFs with well controlled diameter by using the nanocrystalline Fe–Si–B alloy, and to clarify the difference of growth processes of VGCFs between Fe–Si–B and Fe–Zr–B alloys as catalysts.

2. Experimental Procedures

The nanocrystalline Fe–Si–B alloy was prepared by a melt-spinning technique. The composition of $Fe_{75}Si_{15}B_{10}$ was used in this study. The alloy ingot was prepared by arc-melting a mixture of Fe (99.9%), Si (99.5%) and crystalline B (99.5%) in Ar. To obtain melt-spun ribbons, the alloy ingot was then melted and injected onto a Cu roller rotating at a circumferential speed of 42 m/s under Ar. It was confirmed from the X-ray diffraction pattern that the resultant ribbons consisted of an amorphous phase without any crystalline phases including bcc-Fe. To precipitate fine bcc-Fe grains, the as-quenched ribbon samples with a size of about 8×0.02 mm^2 were then annealed at 773 K for 5 min in Ar. The annealed ribbon samples were finally ground into powders with the size of less than 45 μm.

The nanocrystalline $Fe_{75}Si_{15}B_{10}$ alloy powders with fine bcc-Fe grains were placed onto a Pt boat, and introduced into a reactor tube equipped with an infrared lamp. To activate the catalytic function of the alloy, the catalyst powders were reduced under H_2 at 623 K. The temperature was increased up to 773 K or 873 K, and the reactant gas of 80%CO–20%H_2 was then introduced into the reactor tube. The process time varied from 1 to 5 h, while the gas-flow rate of 50 cm^3/min was fixed through this study.

The morphology of the VGCFs was observed by a field-emission-type scanning electron microscopy (FE-SEM, Philips XL-30FEG), a transmission electron microscopy (TEM, JEOL JEM-2000EX II and HITACHI H-800), and a high-resolution electron microscopy (HREM, Philips CM200FEG). The amount of the VGCFs grown on the catalyst powders was measured by thermogravimetry (TG) as a function of reaction time, and the deposition rate was calculated by differentiating the TG data with respect to reaction time.

---

3. Results and Discussion

3.1 Microstructures of Fe–Si–B catalysts

Prior to synthesis of the VGCFs, the microstructure of catalysts was observed. It is well known that the grain size of bcc-Fe precipitated from as-quenched Fe–Si–B depends on the annealing temperatures. To clarify the grain size of bcc-Fe at temperatures of VGCF growth, TEM observations of Fe–Si–B catalysts annealed at 773 K and 873 K were performed.

Figure 1 shows the transmission electron micrographs of the $Fe_{75}Si_{15}B_{10}$ melt spun ribbon annealed at (a) 873 K and (b) 773 K for 5 min in Ar. The annealing temperatures correspond to those of synthesis of VGCFs. The $Fe_{75}Si_{15}B_{10}$ melt-spun sample annealed at 873 K has grains with a diameter of about $100 \sim 200$ nm. The X-ray diffraction pattern revealed that the grains consist of the bcc-Fe, Fe_3B, and Fe_2Si phases. The grain size after annealing at 773 K was found to be about less than 20 nm, and the grains consist of only bcc-Fe phase. These catalysts were used for the synthesis of VGCFs under $80\%CO-20\%H_2$.

3.2 Synthesis of VGCFs

The deposition of carbon on the nanocrystalline $Fe_{75}Si_{15}B_{10}$ alloy powders was observed without magnification after the $80\%CO-20\%H_2$ mixture were given at 773 and 873 K. Figure 2 shows the scanning electron micrograph of the VGCFs grown from the alloy powders at 873 K under the $80\%CO-20\%H_2$ mixture. The carbon, which is recognized as dark contrasts, has a filamentous structure with a diameter ranging from 100 nm to 200 nm. It is obvious that the width of the VGCF is governed by the size of catalyst particle (white

contrast in Fig. 2), and the VGCF is grown in one direction from the catalyst particle. In addition, the size of each catalyst particle embedded in VGCF is consistent with that of bcc-Fe grain precipitated by annealing at 873 K (Fig. 1(a)).

Figure 3 shows SEM micrograph of the carbon taken from the nanocrystalline $Fe_{75}Si_{15}B_{10}$ alloy powders annealed at 773 K for 5 h under the $80\%CO-20\%H_2$ mixture. Although it is difficult to identify the filamentous carbons, the VGCFs with a width less than about 40 nm were formed; the width of VGCFs corresponds to the size of bcc-Fe grain precipitated by annealing at 773 K (Fig. 1(b)) as well as at 873 K. These observations indicate that the VGCFs can grow using the nanocrystalline $Fe_{75}Si_{15}B_{10}$ alloy as a catalyst, and the diameter of VGCFs can be controlled by the grain size of bcc-Fe.

3.3 Structure of VGCFs grown by Fe–Si–B catalysts

To clarify the detailed structure of the VGCFs and catalyst particles, HREM and TEM observations were performed. Figure 4 shows (a) the transmission electron micrograph of the VGCFs grown from the nanocrystalline $Fe_{75}Si_{15}B_{10}$ alloy powders prepared at 873 K under the $80\%CO-20\%H_2$ mixture, (b) the magnified lattice image of the VGCF, and (c) the schematic diagram of the fiber structure,[4] respectively. In Fig. 4(a), it is obvious that the fiber grew from the upper left to the lower right, and there was a catalyst particle, which can be recognized as black contrast, at the tip of the fiber. This VGCF seems to have tubular-type structure, since the contrast of the center part is relatively bright, compared to the edge part. Figure 4(b) shows the magnified image of the marked section in Fig. 4(a). As expected, the VGCF con-
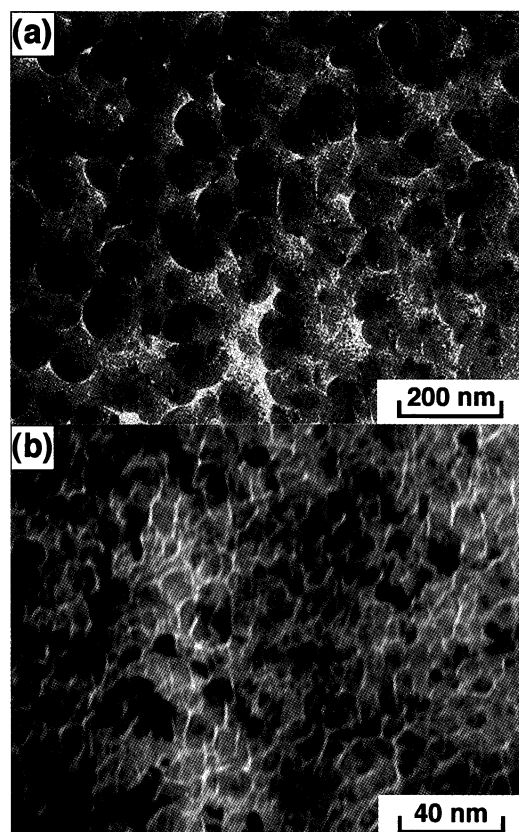

200 nm

40 nm

Fig. 1 Transmission electron micrographs of the $Fe_{75}Si_{15}B_{10}$ melt-spun ribbon annealed at (a) 873 K and (b) 773 K in Ar for 5 min.
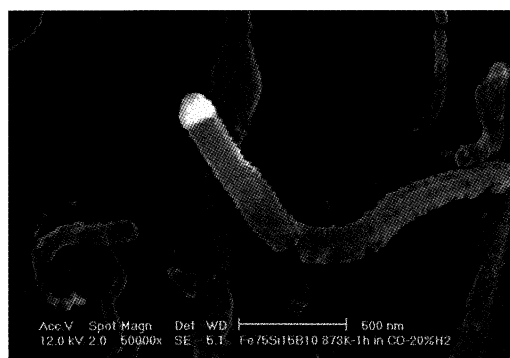

Fig. 2 Scanning electron micrograph taken from the VGCFs grown from the nanocrystalline $Fe_{75}Si_{15}B_{10}$ alloy powders at 873 K for 1 h under the $80\%CO-20\%H_2$ mixture.
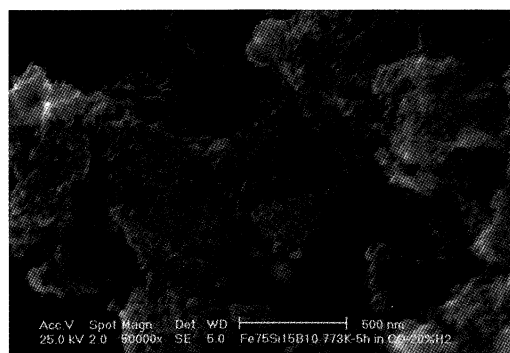

Fig. 3 Scanning electron micrograph taken from the VGCFs grown from the nanocrystalline $Fe_{75}Si_{15}B_{10}$ alloy powders at 773 K for 5 h under the $80\%CO-20\%H_2$ mixture.

Fig. 5   Electron Diffraction pattern of the catalyst particle embedded in the VGCF grown from the nanocrystalline $Fe_{75}Si_{15}B_{10}$ alloy powders annealed at 873 K for 1 h under the 80%CO-20%H_2 mixture.
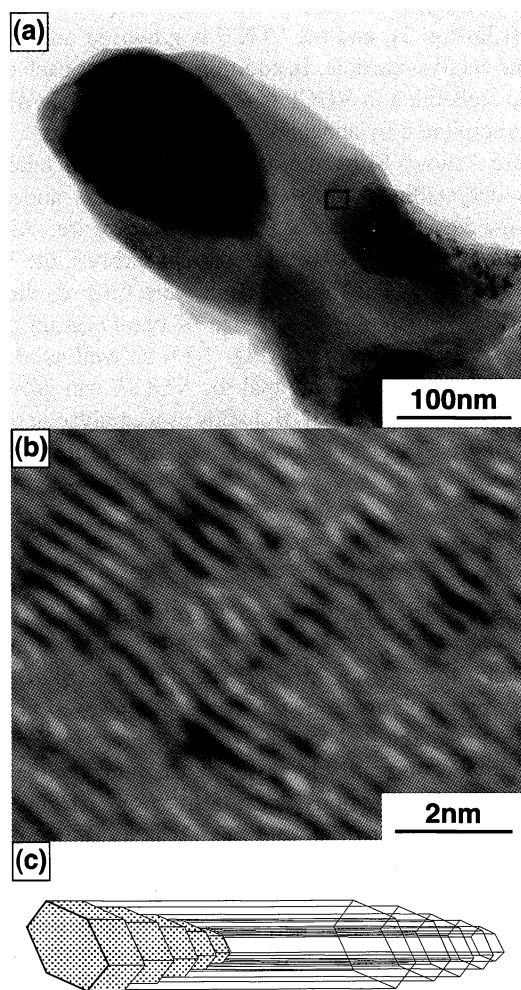
Fig. 4   (a) Transmission electron micrograph taken from the VGCF grown from the nanocrystalline $Fe_{75}Si_{15}B_{10}$ alloy powders annealed at 873 K for 1 h under the 80%CO-20%H_2 mixture, (b) the magnified lattice image of the VGCF, and (c) the schematic diagram of the fiber structure.

Fig. 6   (a) High-resolution electron micrograph taken from the VGCF grown from the nanocrystalline $Fe_{75}Si_{15}B_{10}$ alloy powders annealed at 773 K for 5 h under the 80%CO-20%H_2 mixture, and (b) its magnified image of selected area in (a).

sisted of graphite platelets that were stacked parallel to the fiber axis. This structure is schematically illustrated in Fig. 4(c).

The chemical composition of the catalyst particle was analyzed by energy dispersive spectroscopy (EDS) with a beam-spot size of 100 nm. It turned out that the particle consisted of Fe and C, while Si and B were not detected within the detection limit of the EDS. This implies that the catalyst particle consisted of Fe_3C. To clarify the phase, a diffraction pattern of the catalyst was analyzed. Figure 5 shows the electron diffraction (ED) pattern of the catalyst particle. Since the ED pattern was indexed as Fe_3C single grain (see spots A, B, and C) and Graphite (002), it can be said that the catalyst particle observed at the tip of the fibers was Fe_3C. Sacco and co-workers reported[5] that the bcc-Fe phase changes into the Fe_3C phase. These results obtained in this study show a good agreement with their observations.

The VGCFs grown on the nanocrystalline $Fe_{75}Si_{15}B_{10}$ alloy powders at 773 K were also observed. Figure 6 shows (a) the high-resolution electron micrograph of the VGCFs grown from the nanocrystalline $Fe_{75}Si_{15}B_{10}$ alloy powders at 773 K under the 80%CO-20%H_2 mixture, and (b) its magnified image of the marked section in (a). Judging from Fig. 6(b), the graphite sheets seem to be stacked parallel to the fiber axis at the edges of the fiber. This suggests that the VGCFs grown at
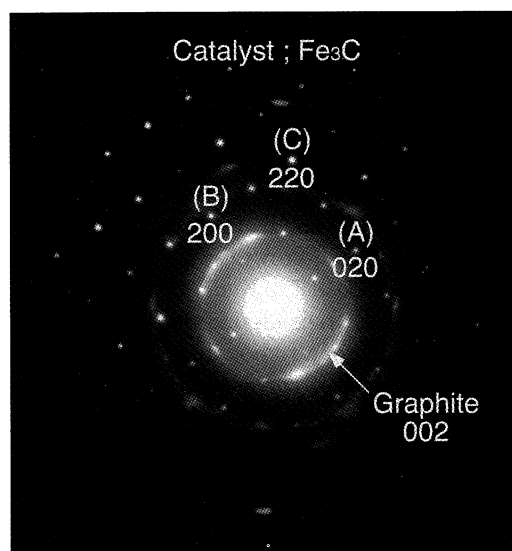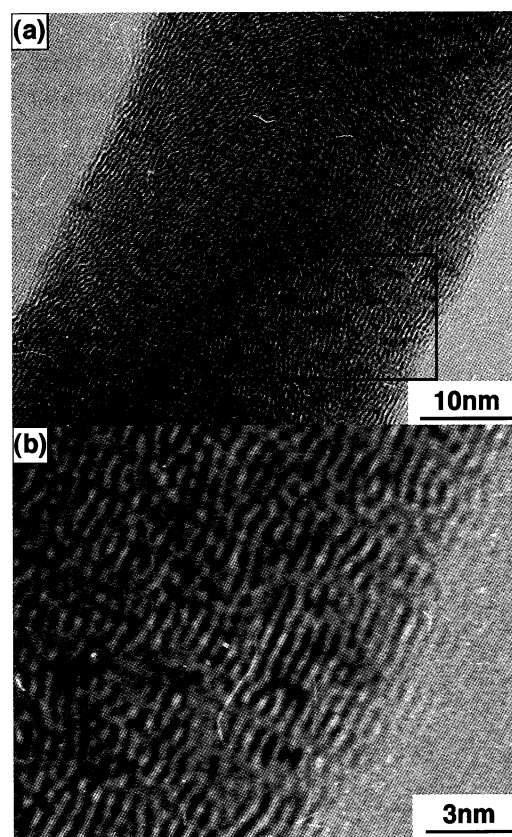
773 K also have a tubular-type structure. Unfortunately, the catalyst particles embedded at the tip of VGCFs could not be observed in this study.

3.4   Growth process of VGCFs

To quantify the growth process of VGCFs, the deposition rate of VGCFs on nanocrystalline $Fe_{75}Si_{15}B_{10}$ catalysts at 873 K under 80%CO-20%H_2 mixture was derived from TG analysis as a function of reaction time, and plotted in
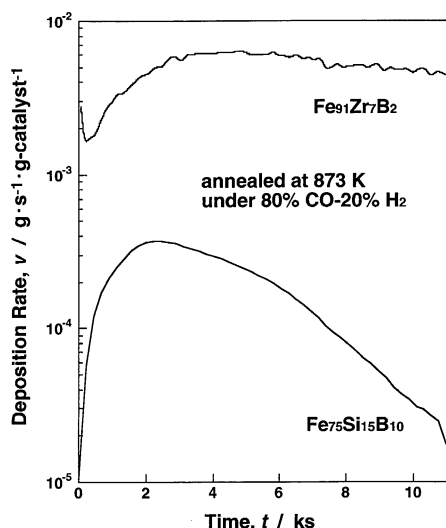
Fig. 7 Deposition rate of the VGCFs grown at 873 K under the 80%CO–20%H$_2$ mixture as a function of reaction time, t.
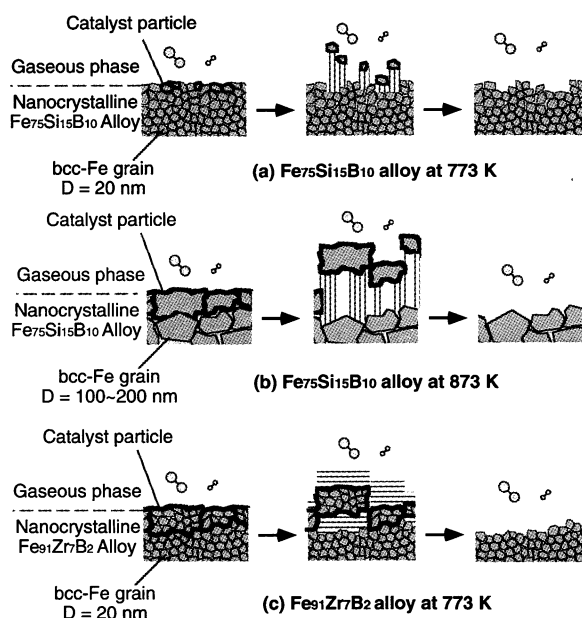

Fig. 8 Schematic diagram of the growth process of VGCFs from the nanocrystalline (a) Fe$_{75}$Si$_{15}$B$_{10}$ alloy at 873 K, (b) Fe$_{75}$Si$_{15}$B$_{10}$ alloy at 773 K, and (c) Fe$_{91}$Zr$_7$B$_2$ at 873 K under the 80%CO–20%H$_2$ mixture.

Fig. 7. In addition, the deposition rate of VGCFs grown from Fe$_{91}$Zr$_7$B$_2$ catalyst was also plotted in Fig. 7 as a reference. It should be noted that the deposition rate was normalized by the mass of catalyst powders.

It is found that two deposition rate curves are resemble each other in shape. At the beginning of the synthesis reaction, the deposition rate increased and showed maximum followed by decrease in the rate with increasing time. The increase in deposition rate at the beginning suggests that the "active" catalyst particles were provided from the larger powder with a diameter of $\sim$ 45 μm. However, once the larger powders were completely broken up into smaller catalyst particles, the rate would decrease since the activity of the catalyst particles is usually degraded with increasing time due to the deposition of unfavorable amorphous carbon on the catalyst surface. Although two curves were resemble in shape, the Fe$_{75}$Si$_{15}$B$_{10}$ catalyst powders tend to show the maximum ear-

lier (2.3 ks from the beginning of synthesis reaction) than the case of Fe$_{91}$Zr$_7$B$_2$ (3.6 ks). This suggests that the Fe$_{75}$Si$_{15}$B$_{10}$ catalyst powders were more fragile and broken easier than the case of Fe$_{91}$Zr$_7$B$_2$.

Even though further investigations should be performed to clarify the growth process, including the analysis of gas composition after the reaction, based on the morphological observation and gravimetric analysis, the proposed growth process of the VGCFs from nanocrystalline Fe$_{75}$Si$_{15}$B$_{10}$ alloy in this study can be schematically illustrated in Fig. 8. To clarify the difference in the growth process between Fe$_{75}$Si$_{15}$B$_{10}$ and Fe$_{91}$Zr$_7$B$_2$, the process for Fe$_{91}$Zr$_7$B$_2$ that was proposed in our work[3] was also depicted in Fig. 8(c). It should be noted that the bcc-Fe phase changed into the Fe$_3$C phase and acted as a catalyst for the carbon deposition and the subsequent filament growth. Unlike the case of Fe$_{91}$Zr$_7$B$_2$, the Fe$_{75}$Si$_{15}$B$_{10}$ catalyst particles embedded in the VGCFs seem to consist of the single Fe$_3$C phase. Because of this, the VGCFs grown from the Fe$_{75}$Si$_{15}$B$_{10}$ catalyst had small diameter and showed relatively homogeneous diameters. It seems that the difference in the way of separation of catalyst particle between Fe$_{75}$Si$_{15}$B$_{10}$ and Fe$_{91}$Zr$_7$B$_2$ alloys was due to the difference in the brittleness of these alloys.

4. Conclusion

The synthesis of vapor-grown carbon fibers (VGCFs) with well controlled diameter by using the nanocrystalline Fe–Si–B alloy as a novel catalyst has been investigated, and the catalytic difference in the growth process of VGCFs for the Fe$_{75}$Si$_{15}$B$_{10}$ alloy and the Fe$_{91}$Zr$_7$B$_2$ alloy as catalysts has been examined.

It was found that the VGCFs can be grown by using the nanocrystalline Fe$_{75}$Si$_{15}$B$_{10}$ alloy as a catalyst, and a diameter of VGCFs can be controlled by the grain size of bcc-Fe. A width of VGCFs grown at 773 K under the 80%CO–20%H$_2$ was less than 40 nm.

From HREM observations, with regard to the structure of VGCFs, it was found that "tubular-type" can be grown at both 773 K and 873 K using the Fe$_{75}$Si$_{15}$B$_{10}$ catalyst

As far as the catalyst particles embedded in VGCFs were concerned, unlike the case of Fe$_{91}$Zr$_7$B$_2$, the Fe$_{75}$Si$_{15}$B$_{10}$ catalyst particle was made of single Fe$_3$C grain. This can be attributed to the brittleness of catalyst particles.

REFERENCES

1) C. Park, N. M. Rodriguez and R. T. K. Baker: J. Catal. **169** (1997) 212–227.
2) C. Park and R. T. K. Baker: J. Catal. **179** (1998) 361–374.
3) K. Unno, H. Kudo, A. Kamegawa, H. Takamura, M. Okada, Y. Watanabe, R. Takahashi and J. Yagi: Mater. Trans., JIM **41** (2000) 563–566.
4) N. M. Rodriguez, Alan Chambers and R. T. K. Baker: Langmuir **11** (1995) 3862–3866.
5) A. Sacco, Jr., P. Thacker, T. N. Chang and A. T. S. Chiang: J. Catal. **85** (1984) 224–236.